

# Numerical Simulations of Gamma-Ray Burst Explosions

Davide Lazzati<sup>a</sup>, Brian J. Morsony<sup>b</sup>, Diego López-Cámara<sup>c</sup>

<sup>a</sup>*Department of Physics, Oregon State University, 301 Weniger Hall, Corvallis, OR 97331, USA*

<sup>b</sup>*Department of Astronomy University of Maryland 1113 Physical Sciences Complex College Park, Md 20742-2421*

<sup>c</sup>*Instituto de Astronomía, Universidad Nacional Autónoma de México, Apdo. postal 70-264 Ciudad Universitaria, D.F., Mexico*

---

## Abstract

Gamma-ray bursts are a complex, non-linear system that evolves very rapidly through stages of vastly different conditions. They evolve from scales of few hundred kilometers where they are very dense and hot to cold and tenuous on scales of parsecs. As such, our understanding of such a phenomenon can truly increase by combining theoretical and numerical studies adopting different numerical techniques to face different problems and deal with diverse conditions. In this review, we will describe the tremendous advancement in our comprehension of the bursts phenomenology through numerical modeling. Though we will discuss studies mainly based on jet dynamics across the progenitor star and the interstellar medium, we will also touch upon other problems such as the jet launching, its acceleration, and the radiation mechanisms. Finally, we will describe how combining numerical results with observations from Swift and other instruments resulted in true understanding of the bursts phenomenon and the challenges still lying ahead.

*Keywords:* Gamma-Ray bursts, Hydrodynamics, Special Relativity, Radiation Mechanisms

---

## 1. Introduction

Numerical simulations have played a major role in the understanding of gamma-ray burst (GRB) studies in the past decade. Even though it is difficult to find a precise moment in which it all begun, the growing evidence of association between long-duration GRBs and core-collapse supernovae in the late 1990s [64, 15, 54, 4] arguably played a major role in supporting the need for theoretical tools that could go beyond the approximations of spherical symmetry and/or top-hat jets. Numerical simulations are now used as a major tool in many aspects of the GRB phenomenology.

First, numerical methods are used to understand the properties of the progenitor. Binary compact mergers are heavily studied as short GRB progenitors [57, 18, 19, 58] and massive, fastly spinning stars and their core-collapse are

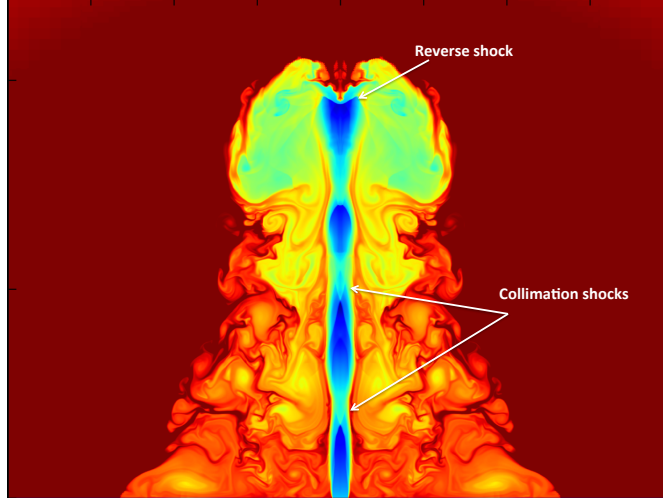


Figure 1: False-color rendering of a relativistic jet expanding in the core of a massive star. Red colors show high-density while blue colors show low-density regions. The reverse shock that decelerates the jet material and the tangential collimation shocks are indicated. The forward bow-shock propagating in the interstellar media is not shown. Adapted from [32].

investigated as potential long GRB progenitors [65, 67, 66]. Numerical simulations are also used to understand the jet launching from a compact object, either a black hole or a magnetar [42, 43, 23, 26, 44, 52, 24, 59, 25, 45]. Subsequently, numerical simulations are used to model the dynamics of both magnetized [7, 8] and unmagnetized jets [40, 1, 68, 69, 46, 50, 47, 51, 35, 49]. Numerical simulations are finally used to model the prompt emission phase [55, 27, 28, 30, 48, 63, 33, 38, 36, 39, 9] and, eventually, the afterglow [60, 13, 14, 61, 62].

In this review we will concentrate on the hydrodynamical aspect of simulations, focusing on the interaction between the jet and the progenitor star and its consequences on the jet dynamics, propagation, and radiation mechanism. We remind the reader to the above references for a more complete discussion of the various numerical techniques and physical problems addressed.

## 2. Inside the star: ploughing through

Hydrodynamical (HD) simulations of relativistic jets inside massive stars have played a major role in our understanding of the GRB phenomenology. They are based on the assumption that somehow the central engine - being a black hole or a magnetar - is capable of producing a jet with the adequate luminosity and entropy. The jet has to propagate through a star that is mostly unchanged since core-collapse, its free-fall time being longer than the typical GRB duration at radii beyond  $\sim 10^9$  cm from the star's center. More controversial is the jet

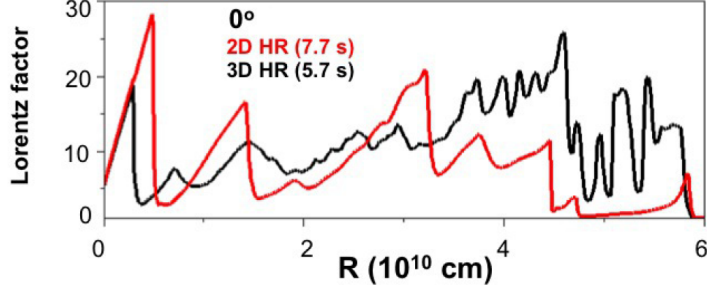


Figure 2: Radial profile of the Lorentz factor of jets propagating in massive stars at the time of their breakout off the star’s surface. Results from a 2D simulation (red) and a 3D simulation (Black) are compared, showing how 3D produces a more complex profile due to the presence of multiple minor shocks rather than a few strong ones. Adapted from [35].

composition at the jet’s base, i.e. the inner boundary of the simulation. Most simulations are HD and ignore the presence of magnetic fields. This is a good approximation as long as the magnetization is low. Since most jet launching mechanisms are heavily based on strong magnetization, such an assumption has unclear validity. Simulating unmagnetized jets, on the other hand, makes it possible to satisfy the requirement of very high resolution in the boundaries between the relativistic outflow and the surrounding star, a resolution that can be achieved only with adaptive mesh techniques.

The first issue numerical simulations have to address is the propagation of the jet inside the star. A known result is that the jet cannot expand conically and accelerate proportionally to the radius inside the progenitor star [41]. Early GRB simulations [40, 1] showed that the jet head propagates trans-relativistically, at few tens of per cent of the speed of light. This speed depends very weakly on the jet and star properties and a value  $\beta_h = 0.25$  for the jet-head speed gives an accurate prescription for the propagation inside the star [32]. A sub-luminal propagation speed also ensures that the jet is causally connected with the star and the star material that accumulates in front of the jet can move aside. Numerical results can be qualitatively reproduced by analytical models [50, 5, 6]. Even the most advanced analytical models, however, assume cylindrical symmetry and do not include important effects such as vortex shedding, multiple tangential shocks, and turbulence. As a consequence, they cannot exactly reproduce some simulations detail and fail to precisely predict even the jet head expansion velocity inside the progenitor star [32].

One important consequence of a relatively slow jet propagation inside the star is the creation of a cocoon that surrounds the jet. An amount of energy

$$E_{\text{Cocoon}} = L_j \left( t_{\text{bo}} - \frac{R_\star}{c} \right) \sim L_j \frac{R_\star}{c\beta_h} = 10^{52} L_{j,51} R_{\star,11} \text{ erg} \quad (1)$$

is deposited in the cocoon and, from the cocoon, is transferred to the star.  $L_j$  is the engine luminosity,  $t_{\text{bo}}$  is the jet breakout time,  $R_\star$  is the progenitor star’s

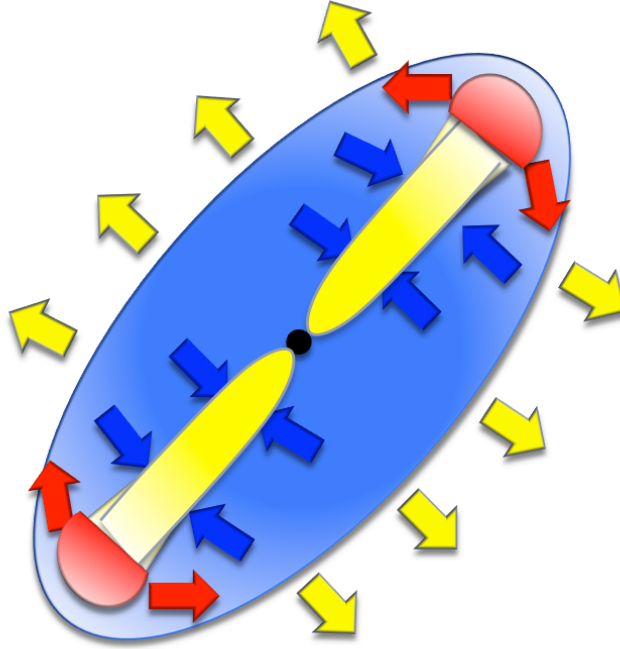


Figure 3: Cartoon of the jet propagation dynamics inside a massive star. The jet (yellow) is launched. It pushes against the star material and a bow shock (Red) develops, shoving hot jet and star material to the side, feeding a uniform pressure cocoon (blue). The cocoon pressure pushes against the star, unbinding it, and the jet, collimating it into a smaller angle.

radius, and  $\beta_h$  is the jet's head propagation speed in units of the speed of light.  $L_{j,51}$  and  $R_{*,11}$  are the luminosity and stellar radius normalized by  $10^{51} \text{ erg s}^{-1}$  and  $10^{11} \text{ cm}$ , respectively. Note that once the jet head has broken out onto the star's surface, all the jet behind the head does exit the star, accounting for the  $R_*/c$  term in the equation above. The energy deposited in the cocoon is therefore enough to unbind the stellar material. However, because the jet deposits the energy in the star far from the core, the explosion might be darker than a normal core-collapse supernova (CCSN). This is due to the lack of newly synthesized  $^{56}\text{Ni}$ , whose decay powers the light curve of “normal” CCSNe. The presence of jets, however, changes the energy distribution in the ejecta, producing explosions with fast ejecta that can explain bright radio emission in some supernovae [32].

A firm result of simulations, independent of the code and of the jet and star properties, is the complexity of the jet profile. The jet is characterized by the presence of multiple shocks (Figure 1). There is a reverse shock that decelerates the expanding jet as a consequence of the bow shock at the jet's head. There are,



Figure 4: Volume rendering of the velocity of a long GRB jet as it erupts off the surface of the progenitor star.

however, several collimation shocks behind the reverse shock as well. These are tangential shocks that are produced by the interaction of the jet with the cocoon. As a consequence of the presence of collimation shocks the jet’s Lorentz factor is not uniform behind the reverse shock, but it has a characteristic sawtooth shape (Figure 2). A cartoon showing the various components of the jet-star interaction dynamics is shown in Figure 3.

Initial simulations of the jet propagation were performed in cylindrical symmetry in two dimensions [40, 1, 50]. More recently, full 3D simulations have become possible. They show interesting features and more complexity in the jet dynamics. One important limitation of 2D simulations is the “plug instability”, an effect whereby any overdensity of ambient medium that accumulates ahead of the jet next to the axis is trapped and creates an obstacle. As a consequence the system develops two plumes of low-density, high-temperature material at large polar angles (see, e.g., Figure 1 in Lazzati et al. [29]). This instability is seen in jets from both constant and variable engines [36]. 3D simulations have shown that the jet, instead, travel through the path of least resistance, its head moving round the polar axis to avoid over-densities in the progenitor star or induced by the bow shock itself [69, 35]. As a consequence, the collimation shocks are also reduced in size and intensity, producing a more complex structure and a smoother profile of the Lorentz factor (Figures 2, 4).

### 3. Outside the star: free expansion...almost

A second important stage of a GRB jet is its expansion once it has left the progenitor star. The jet is expected to be freely expanding at this point, accelerating proportionally to its radius until reaching the asymptotic Lorentz factor of several hundreds (e.g., [56]). However, simulations have shown that the interactions with the stellar material carries on after the jet has left the star. External material is provided by the expanding cocoon that propagates out of

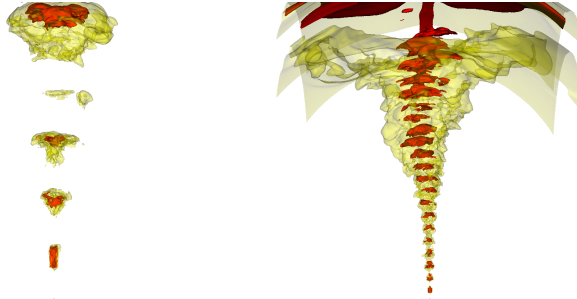


Figure 5: Comparison between the evolution of jets from engines with different dead times. Red colors show relativistic expansion, while yellow colors show mildly relativistic expansion. The jet on the left is produced by an engine with activity and dead times of 0.5 seconds. The jet on the right is produced by an engine with activity and dead times of 0.1 seconds.

the star at close to the speed of light but has a significantly higher density than the jet. This causes the jet to accelerate at a significantly slower rate than a free-expanding jet and ensures the survival of tangential collimation shocks well beyond the stellar surface [27]. It has also been shown that the interaction of the star with the jet can imprint new variability features on the jet, especially for long lived engines.

Simulations of variable GRB jets have been performed in 2D [51, 36] and, more recently in 3D (Lazzati et al. in preparation). They show that the jet star interaction can work in different ways, depending on the time-scale of the variability.

- If the engine is characterized by very long time-scale variability, longer than a few seconds, the interaction with the star does not affect the long-term variability, but adds a few-second timescale to the jet energy outflow [51].
- If the engine has very high frequency variability (faster than a few tens of Hz), this is left almost unmodified by the jet propagation through the progenitor and can be translated, almost pulse to pulse, in the jet luminosity profile [51].
- If the engine has variability on time-scales of seconds, they interact destructively with the progenitor star variability timescale. For a variable jet that is able to break out of the star, the first active periods are destroyed as they create the funnel through the stellar progenitor [36]. A set of 3D simulations was performed to investigate the role of jet variability in the stability of jet propagation. It showed that in the cases in which the dead times of the jet are of the order of  $\sim 1$  seconds, the star has time to close the funnel previously dug by the jet. As a consequence, energy has to be spent again in reopening the channel and the duration of activity times, as seen by a distant observer, is reduced (Lazzati et al. in preparation). A

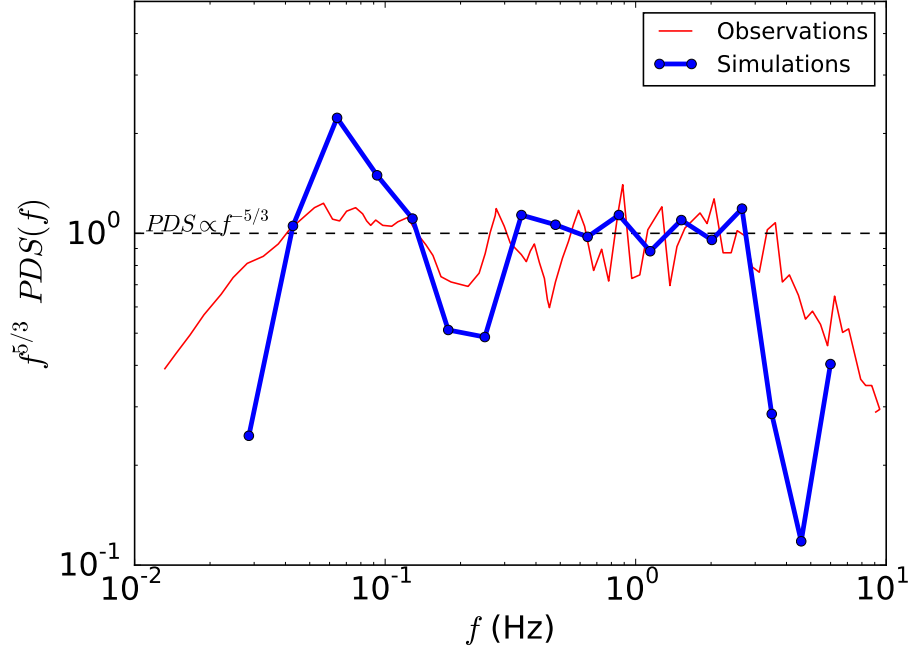


Figure 6: Comparison between the average power density spectrum of a sample of BATSE GRBs [3] and the average power density spectrum of synthetic light curves from hydrodynamic simulation of GRB jets [51].

comparison between the jet of an engine with 0.5 s dead times and the jet of an engine with 0.1 s dead times is shown in Figure 5. while the jet from the engine with faster variability preserves the duration of the active and dead times (equal spacing and durations of red and yellow phases), the jet from an engine with longer dead times needs to use the energy of the active pulses to re-open the funnel. As a consequence active pulses reach the star surface with significantly reduced duration producing an asymmetry between active and dead times in the jet luminosity at large radii. Such an asymmetry is imprinted in the light curve as well, and could explain the detection of longer than usual dead times in some long-duration BATSE GRBs [53].

A significant result of these simulations is the fact that the resulting light curves have variability properties analogous to the ones of observed GRBs [51, 36]. Figure 6 shows a comparison between the power spectrum of light curves from 2D HD simulations and those of observed BATSE long-duration GRBs. Simulations reproduce the average slope ( $\propto \nu^{-5/3}$ ), the low frequency cut-off and the high-energy cutoff seen in observations. Especially the low-frequency cut-off, entirely set by the interaction with the progenitor star, is significative of the role of the star in shaping the light curve of bursts.

Finally, the jet star interaction might be responsible for X-ray flares in the light curve of burst afterglows [10]. Any instability in the jet pressure against the star is amplified by the star's response, leading to a time-duration correlation consistent with observations [31].

#### 4. The radiative stage and ensemble correlations

The radiation mechanism of GRBs is perhaps still the most controversial aspect of the whole phenomenon. The standard view of a synchrotron-dominated spectrum [56] is giving way to a more elaborated scenario in which advected radiation released at the photosphere dominates or, at least, contributes substantially to the light curve energy budget [55, 22, 33]. Within this scenario, meaningful light curves and spectra can be straightforwardly calculated from the results of numerical simulations [27, 48, 11, 12]. The underlying assumption is that radiation and matter are in equilibrium until some radius in the sub-photospheric region where they decouple and evolve independently thereafter. Assuming also that the radiation has a thermal spectrum, the bolometric luminosity and peak frequency of the emission can be extracted from local HD quantities (energy density) and boosted to the observer frame given the local velocity.

Such simulations have been very successful in reproducing ensemble results of GRB emission based on a very few assumptions on the properties of the progenitor stars and their central engines. The Amati correlation [2] was shown to be reproduced as an effect of the viewing angle, robust to changes of jet and progenitor star properties [27, 33]. The same set of simulations reproduced the Lorentz factor-isotropic energy correlation [34, 17] and predicted the existence of a correlation between radiation efficiency and peak frequency, later found in Swift data. The three observational correlations are shown in Figure 7 with the theoretical data overlaid. Another correlation that can be explained from simulations within the photospheric scenario is the Golenetskii correlation [36], the correlation between the peak energy and the luminosity in finite intervals of GRB light curves [21, 16, 37]. This correlation is particularly significant given the debate over the reliability of the Amati correlation. A set of simulations with intermittent engines showed that the general behavior of the Golenetskii correlation could also be produced, albeit with a marginal offset in normalization (Figure 8).

#### 5. Spectral calculations

Despite all the success seen above, radiation codes coupled to numerical simulations cannot relax the assumption of thermal equilibrium and cannot therefore reproduce the broad-band non-thermal character of observed GRB spectra. Detailed spectral models come therefore from one-zone simulations in which the diversity of the dynamic conditions seen in HD simulations is neglected in favor of a more detailed spectral modeling. In some cases, one



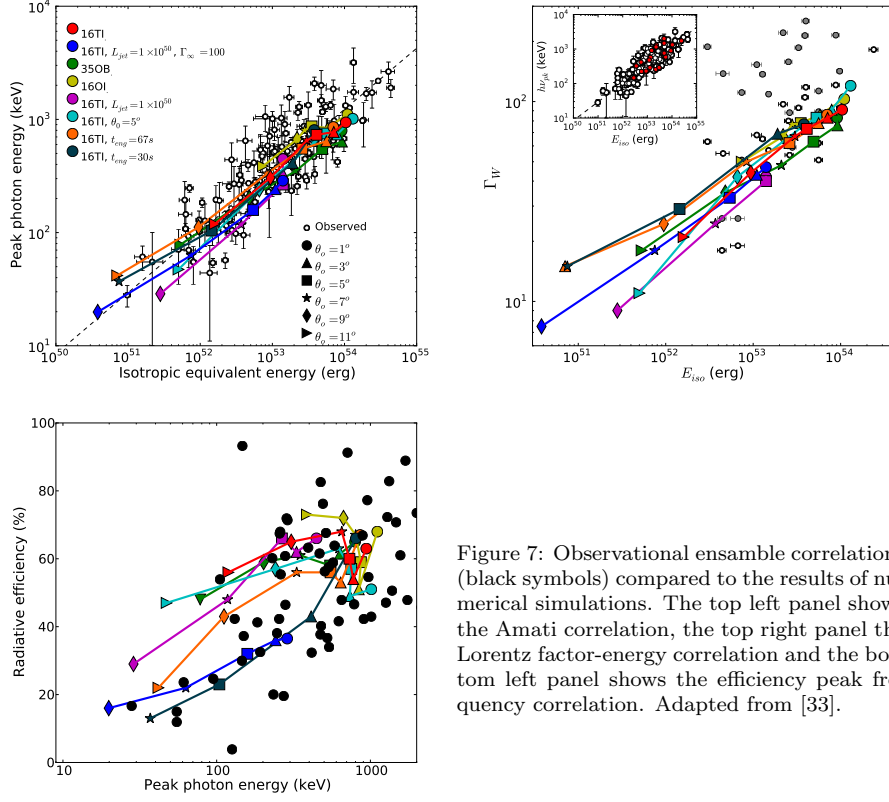


Figure 7: Observational ensemble correlations (black symbols) compared to the results of numerical simulations. The top left panel shows the Amati correlation, the top right panel the Lorentz factor-energy correlation and the bottom left panel shows the efficiency peak frequency correlation. Adapted from [33].

dimension of complexity is maintained, assuming a radial evolution of the jet in free expansion [55, 20]. In other cases, more sophisticated radiation treatment can be applied only to a single zone [9].

Figure 9 shows the results of Monte Carlo simulations of the radiation-matter relaxation following an event of sudden energy dissipation in the lepton population. The relaxation is assumed to be dominated by Compton and inverse Compton scattering and by pair creation and annihilation. Calculations like these are necessary since GRB jets at the photosphere are radiation dominated and one cannot assume that the electron have a well defined temperature. As seen in Figure 9, both the photon and the electron energy distributions have a markedly non-thermal character in the transition period while equilibrium is restored. Since the scattering take place in a relativistically expanding medium, in which photons and electrons propagate at very small angle, the scattering rate is greatly inhibited and the non-thermal phase can last for a significant amount of time.

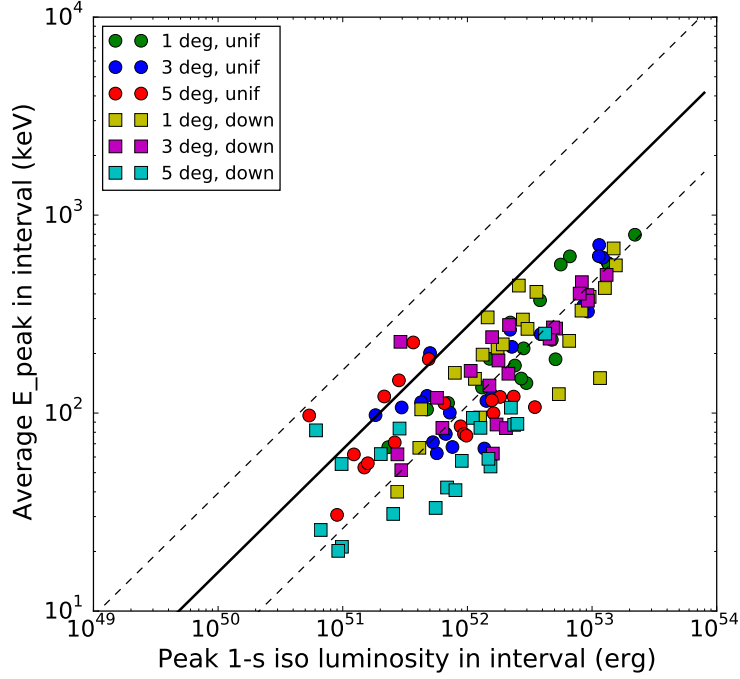


Figure 8: Golenetskii correlation. Results from numerical simulations (colored symbols) are overlaid on the best-fit observational correlation (solid line) and its 2-sigma uncertainty region (dashed lines). Adapted from [36].

## 6. Summary and conclusions

In summary, numerical simulations of GRB outflows have allowed us to gain a much deeper insight in the phenomenon. Comparisons with large sample of data such as the BATSE and Swift catalogs have been pivotal in refining the parameters and physics that is needed to explain GRB observations. In this review we concentrated on the HD aspect of the GRB phenomenon and briefly touched on the prompt radiation phase. Other phases, progenitor, central engine, and afterglow have also benefited from numerical studies and we remind the readers to the extensive literature cited in the Introduction for a complete review of numerical studies of GRBs.

## 7. Acknowledgements

This research was partially supported by the Fermi GI program grant NNX12AO74G and Swift GI program grant NNX13A095G (DL and DLC). BJM is supported by an NSF Astronomy and Astrophysics Postdoctoral Fellowship under award AST-1102796.

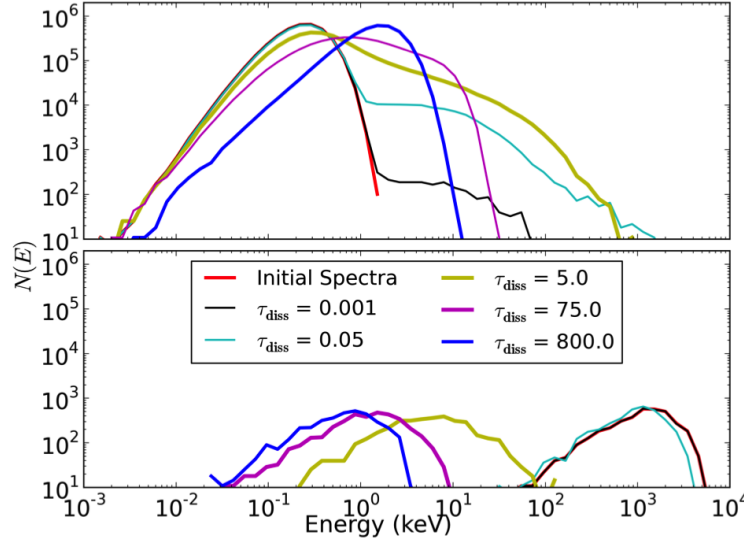


Figure 9: Monte Carlo simulations of radiation-lepton relaxation following the sudden energization of the leptons by a dissipation event in a scattering dominated medium.

## References

- [1] Aloy, M. A., et al., 2000, ApJ, 531, L119
- [2] Amati, L., Frontera, F., Tavani, M., et al. 2002, A&A, 390, 81
- [3] Beloborodov, A. M., Stern, B. E., & Svensson, R. 1998, ApJ, 508, L25
- [4] Bloom J. S., et al., 1999, Nature, 401, 453
- [5] Bromberg, O., & Levinson, A. 2007, ApJ, 671, 678
- [6] Bromberg, O., Nakar, E., Piran, T., & Sari, R. 2011, ApJ, 740, 100
- [7] Bucciantini, N., et al., 2009, MNRAS, 396, 2038
- [8] Bucciantini, N., et al., 2012, MNRAS, 419, 1537
- [9] Chhotray, A., & Lazzati, D., 2015, ApJ in press (arXiv:1502.03055)
- [10] Chincarini, G., Moretti, A., Romano, P., et al. 2007, ApJ, 671, 1903
- [11] Cuesta-Martínez, C., Aloy, M. A., & Mimica, P. 2015, MNRAS, 446, 1716
- [12] Cuesta-Martínez, C., Aloy, M. A., Mimica, P., Thöne, C., & de Ugarte Postigo, A. 2015, MNRAS, 446, 1737
- [13] De Colle, F., Granot, J., López-Cámara, D., & Ramirez-Ruiz, E. 2012, ApJ, 746, 122

- [14] De Colle, F., Ramirez-Ruiz, E., Granot, J., & Lopez-Camara, D. 2012, *ApJ*, 751, 57
- [15] Galama T. J., et al., 1998, *Nature*, 395, 670
- [16] Ghirlanda, G., Nava, L., & Ghisellini, G. 2010, *A&A*, 511, AA43
- [17] Ghirlanda, G., Nava, L., Ghisellini, G., et al. 2012, *MNRAS*, 420, 483
- [18] Giacomazzo, B., Perna, R., 2012, *ApJ*, 758, L8
- [19] Giacomazzo, B., Perna, R., Rezzolla, L., Troja, E., Lazzati, D., 2013, *ApJ*, 762, L18
- [20] Giannios, D. 2006, *A&A*, 457, 763
- [21] Golenetskii, S. V., Mazets, E. P., Aptekar, R. L., & Ilinskii, V. N. 1983, *Nature*, 306, 451
- [22] Guiriec, S., Connaughton, V., Briggs, M. S., et al. 2011, *ApJ*, 727, LL33
- [23] Harikae, S., Takiwaki, T., & Kotake, K. 2009, *ApJ*, 704, 354
- [24] Harikae, S., Kotake, K., Takiwaki, T., & Sekiguchi, Y.-i. 2010, *ApJ*, 720, 614
- [25] Janiuk, A., Mioduszewski, P., & Moscibrodzka, M. 2013, *ApJ*, 776, 105
- [26] Komissarov, S. S., & Barkov, M. V. 2009, *MNRAS*, 397, 1153
- [27] Lazzati D., Morsony B. J., Begelman M. C., 2009, *ApJ*, 700, L47
- [28] Lazzati, D., & Begelman, M. C. 2010, *ApJ*, 725, 1137
- [29] Lazzati, D., Morsony, B. J., & Begelman, M. C. 2010, *ApJ*, 717, 239
- [30] Lazzati, D., Morsony, B. J., & Begelman, M. C. 2011, *ApJ*, 732, 34
- [31] Lazzati, D., Blackwell, C. H., Morsony, B. J., & Begelman, M. C. 2011, *MNRAS*, 411, L16
- [32] Lazzati, D., Morsony, B. J., Blackwell, C. H., & Begelman, M. C. 2012, *ApJ*, 750, 68
- [33] Lazzati, D., Morsony, B. J., Margutti, R., & Begelman, M. C. 2013, *ApJ*, 765, 103
- [34] Liang, E.-W., Yi, S.-X., Zhang, J., et al. 2010, *ApJ*, 725, 2209
- [35] López-Cámara, D., Morsony, B. C., Begelman, M., Lazzati, D., 2013, *ApJ*, 767, 19
- [36] López-Cámara, D., Morsony, B. J., & Lazzati, D. 2014, *MNRAS*, 442, 2202

- [37] Lu, R.-J., Wei, J.-J., Liang, E.-W., et al. 2012, *ApJ*, 756, 112
- [38] Lundman, C., Pe’er, A., & Ryde, F. 2013, *MNRAS*, 428, 2430
- [39] Lundman, C., Pe’er, A., & Ryde, F. 2014, *MNRAS*, 440, 3292
- [40] MacFadyen, A. I., Woosley, S. E., 1999, *ApJ*, 524, 262
- [41] Matzner, C. D. 2003, *MNRAS*, 345, 575
- [42] McKinney, J. C., & Narayan, R. 2007, *MNRAS*, 375, 513
- [43] McKinney, J. C., & Narayan, R. 2007, *MNRAS*, 375, 531
- [44] McKinney, J. C., & Blandford, R. D. 2009, *MNRAS*, 394, L126
- [45] McKinney, J. C., Tchekhovskoy, A., & Blandford, R. D. 2013, *Science*, 339, 49
- [46] Mizuta, A., Yamasaki, T., Nagataki, S., & Mineshige, S. 2006, *ApJ*, 651, 960
- [47] Mizuta, A., & Aloy, M. A. 2009, *ApJ*, 699, 1261
- [48] Mizuta, A., Nagataki, S., & Aoi, J. 2011, *ApJ*, 732, 26
- [49] Mizuta, A., & Ioka, K. 2013, *ApJ*, 777, 162
- [50] Morsony, B. J., Lazzati, D., Begelman, M. C., 2007, *ApJ*, 665, 569
- [51] Morsony, B. J., Lazzati, D., Begelman, M. C., 2010, *ApJ*, 723, 267
- [52] Nagataki, S. 2009, *ApJ*, 704, 937
- [53] Nakar, E., & Piran, T. 2002, *MNRAS*, 331, 40
- [54] Paczynski, B., 1998, *ApJ*, 494, L45
- [55] Pe’er, A., Mészáros, P., & Rees, M. J. 2006, *ApJ*, 642, 995
- [56] Piran, T. 1999, *Physics Reports*, 314, 575
- [57] Rosswog, S., 2007, *MNRAS*, 376, L48
- [58] Rosswog, S., Piran T., Nakar, E., *MNRAS*, 430, 2585
- [59] Taylor, P. A., Miller, J. C., & Podsiadlowski, P. 2011, *MNRAS*, 410, 2385
- [60] van Eerten, H. J., Meliani, Z., Wijers, R. A. M. J., & Keppens, R. 2011, *MNRAS*, 410, 2016
- [61] van Eerten, H. J., & MacFadyen, A. I. 2012, *ApJ*, 751, 155
- [62] van Eerten, H. J., & MacFadyen, A. I. 2013, *ApJ*, 767, 141

- [63] Vurm, I., Beloborodov, A. M., & Poutanen, J. 2011, ApJ, 738, 77
- [64] Woosley, S. E., 1993, ApJ, 405, 273
- [65] Woosley, S. E., Heger, A., 2006, ApJ, 637, 914
- [66] Woosley, S. E., Heger, A., 2006, ApJ, 752, 32
- [67] Yoon, S.-C., Langer, N., Norman, C., 2006, A&A, 460, 199
- [68] Zhang, W., Woosley, S. E., MacFadyen, A. I., 2003, ApJ, 586, 356
- [69] Zhang, W., Woosley, S. E., Heger, A., 2004, ApJ, 608, 365